Autophagy

Autophagy

ISSN: (Print) (Online) Journal homepage: https://www.tandfonline.com/loi/kaup20

Sensitive imaging of Endoplasmic reticulum (ER) autophagy with an acidity-reporting ER-Tracker

Yilong Shi, Xiaoxue Zou, Xianghui Zheng, Yimin Wu, Jiahuai Han & Shoufa Han

To cite this article: Yilong Shi, Xiaoxue Zou, Xianghui Zheng, Yimin Wu, Jiahuai Han & Shoufa Han (2023) Sensitive imaging of Endoplasmic reticulum (ER) autophagy with an acidity-reporting ER-Tracker, Autophagy, 19:7, 2015-2025, DOI: 10.1080/15548627.2023.2165759

To link to this article: https://doi.org/10.1080/15548627.2023.2165759

AUTOPHAGY
2023, VOL. 19, NO. 7, 2015–2025
https://doi.org/10.1080/15548627.2023.2165759

Taylor & Francis
Taylor & Francis Group

RESEARCH PAPER

Sensitive imaging of Endoplasmic reticulum (ER) autophagy with an acidity-reporting ER-Tracker

Yilong Shi[a‡], Xiaoxue Zou[a‡], Xianghui Zheng[b], Yimin Wu[a], Jiahuai Han[c], and Shoufa Han[a]

[a]State Key Laboratory for Physical Chemistry of Solid Surfaces, the Key Laboratory for Chemical Biology of Fujian Province, the MOE Key Laboratory of Spectrochemical Analysis & Instrumentation, and Department of Chemical Biology, College of Chemistry and Chemical Engineering, Xiamen University, Xiamen, China; [b]Bioluminor Biotech Ltd, Xiamen, China; [c]State Key Laboratory of Cellular Stress Biology, Innovation Center for Cell Signalling Network, School of Life Sciences, Xiamen University, Xiamen, China

ABSTRACT

Macroautophagic/autophagic turnover of endoplasmic reticulum (reticulophagy) is critical for cell health. Herein we reported a sensitive fluorescence-on imaging of reticulophagy using a small molecule probe (ER-proRed) comprised of green-emissive fluorinated rhodol for ER targeting and nonfluorescent rhodamine-lactam prone to lysosome-triggered red fluorescence. Partitioned in ER to exhibit green fluorescence, ER-proRed gives intense red fluorescence upon co-delivery with ER into acidic lysosomes. Serving as the signal of reticulophagy, the turning on of red fluorescence enables discernment of reticulophagy induced by starvation, varied levels of reticulophagic receptors, and chemical agents such as etoposide and sodium butyrate. These results show ER probes optically activatable in lysosomes, such as ER-proRed, offer a sensitive and simplified tool for studying reticulophagy in biology and diseases.

Abbreviations: Baf-A1, bafilomycin A_1; CCCP, carbonyl cyanide *m*-chlorophenyl hydrazone; CQ, chloroquine diphosphate; ER, endoplasmic reticulum; FHR, fluorinated hydrophobic rhodol; GFP, green fluorescent protein; Reticulophagy, selective autophagy of ER; RFP, red fluorescent protein; ROX, X-rhodamine; UPR, unfolded protein response

ARTICLE HISTORY
Received 16 May 2022
Revised 30 December 2022
Accepted 3 January 2023

KEYWORDS
Autophagy imaging; endoplasmic reticulum; fluorescence-on; lysosomal acidity; reticulophagy

Introduction

Endoplasmic reticulum (ER) is a membrane-enclosed tubular organelle mediating myriad cell events ranging from protein processing, folding and trafficking to metabolism and to ion storage [1]. Disruption on ER homeostasis is engaged in diverse pathological disorders such as ER stress-associated diseases [2–6]. Selective autophagic removal of excessive or damaged ER (reticulophagy) is recently identified to be executed by a set of specific receptors such as RETREG1/FAM134B [7–9], TEX264 [10] and SEC62 [11,12]. Given the causal role of deregulated ER catabolism in human diseases [2,3,13], methods for sensitive imaging of reticulophagy are of significance to explore the pathophysiological roles of reticulophagy [14] and for development of reticulophagy-inducing drugs [5].

To date, reticulophagy has been assayed by examining altered levels of ER proteins [9,15,16], or with fluorescent proteins with signal peptides specific for ER (such as ss-RFP-GFP-KDEL) [10,12,15]. The former is of low sensitivity as the total ER mass overwhelms that consumed in autophagy and therefore changes on the levels of ER proteins are usually subtle upon reticulophagy [17], while the latter is rather lengthy and inapplicable to primary cells. Essential for cell homeostasis [18], autophagy is a highly conserved pathway that delivers organelles into acidic lysosomes for degradation [19]. Imaging of mitophagy has been successfully achieved with mitochondrion-targeted bio- or chemical probes that could be optically activated in acidic lysosomes [20–27]. In contrast to the diverse imaging agents developed for mitophagy [20–27], the lack of synthetic probes for reticulophagy promotes us to develop a fluorescence-on probe for sensitive detection of reticulophagy. As such, we envisioned that combination of an ER-trappable entity with an acidity-reporting entity might afford a novel ER-Tracker fluorogenic to lysosomes, thus suitable for sensitive imaging of reticulophagy via switched-on fluorescence.

Fluorinated hydrophobic rhodol (FHR) is a green-emissive fluorophore specific for ER [28–30]. The derivative of X-rhodamine with an intramolecular siprolactam (ROX-lactam) is a highly sensitive profluorophore that gives acidity-triggered red fluorescence in lysosomes [31–33]. On the basis of these findings, we hence synthesized ER-proRed, a bifunctional probe containing FHR for ER targeting, and ROX-lactam fluorogenic to lysosomal acidity (Figure 1A). Located in ER, ER-proRed emits green fluorescence. Upon

CONTACT Shoufa Han shoufa@xmu.edu.cn State Key Laboratory for Physical Chemistry of Solid Surfaces, The Key Laboratory for Chemical Biology of Fujian Province, The MOE Key Laboratory of Spectrochemical Analysis & Instrumentation, and Department of Chemical Biology, College of Chemistry and Chemical Engineering, Xiamen University; Xiamen 361005, China; Jiahuai Han jhan@xmu.edu.cn State Key Laboratory of Cellular Stress Biology, Innovation Center for Cell Signalling Network, School of Life Sciences, Xiamen University, Xiamen, China
‡Both authors contributed equally to this work.

Supplemental data for this article can be accessed online at https://doi.org/10.1080/15548627.2023.2165759

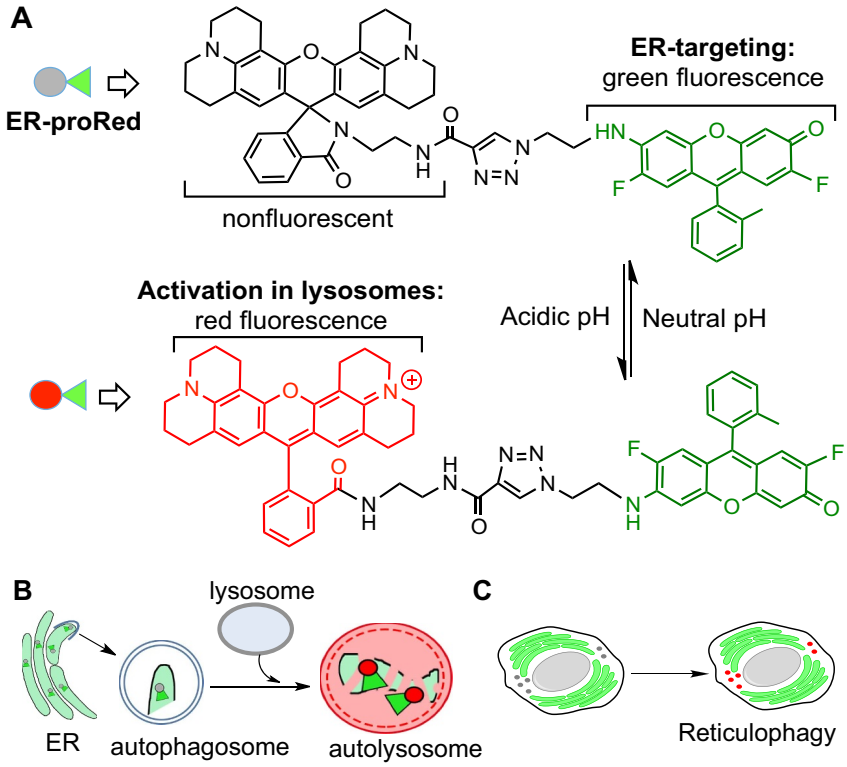

Figure 1. Schematic for fluorescence-on imaging of reticulophagy with ER-proRed. (A) Lysosomal acidity-triggered fluorogenic opening of ROX-lactam of ER-proRed gives bright red fluorescence. (B) Schematic for genesis of red fluorescence upon co-delivery of ER-proRed with ER into acidic lysosomes. (C) Schematic for lysosome-associated red fluorescence of ER-proRed as the reporter of reticulophagy.

reticulophagy, ER fragments and ER-proRed are co-sequestered into autophagosomes. Subsequent fusion of the autophagosomes with acidic lysosomes activates ROX-lactam of ER-proRed, giving rise to red fluorescence (Figure 1B). The level of red fluorescence thus serves as the readout of reticulophagy (Figure 1C). With ER-proRed, reticulophagy was differentiated in cells subjected to starvation, altered expression of reticulophagic receptors, and a variety of chemical stressors.

Results and discussion

Synthesis and characterization of ER-proRed

ER-proRed was readily synthesized via Cu(I)-catalyzed azide-alkyne cyclization between azide-containing FHR and alkyne-tagged ROX-lactam (Fig. S1A). To examine its pH responsiveness, we recorded fluorescence emission of ER-proRed dissolved in buffer of varied pH. This revealed that ER-proRed exhibited pH-inert green fluorescence peaked at 525 nm (FHR) and red fluorescence maximal at 605 nm that was generated in acidic pH and intensified as pH decreased (Figure 2A-B). Genesis of red fluorescence in acidic media is consistent with protonation elicited fluorogenic isomerization of ROX-lactam (Figure 1). ER-proRed exhibited optimal red fluorescence emission in the range of pH 4–5 (Figure 2C-D), which overlaps the window of lysosomal acidity, indicating the feasibility of turn-on red fluorescence of ER-proRed upon delivery into lysosomes.

Selectivity of ER-proRed for endoplasmic reticulum

To verify probe selectivity for ER, ER-proRed was applied to HeLa cells expressing ss-RFP-KDEL, a red fluorescence protein (RFP) with N-terminal signal sequence calreticulin (ss) and C-terminal ER retention sequence KDEL for targeting and retention in ER [34] (Figure 3A). Confocal microscopic analysis showed colocalization of green signals of ER-proRed with red fluorescence of ss-RFP-KDEL with a Pearson's correlation coefficient (PCC) of 0.81 and Manders' tM2 of 0.939 (Figure 3B). We then co-stained HeLa cells with ER-proRed and ER-Tracker Red which is a commercial dye specific for ER. Analysis of ER-Tracker Red and green fluorescence of ER-proRed gave a PCC of 0.85 and Manders' tM2 of 0.985 (Figure 3C), suggesting significant colocalization of ER-proRed with ER-Tracker Red. Furthermore, we observed no detectable ER-proRed in lysosomes (PCC = 0.4 with LysoTracker Red), mitochondria (PCC = 0.28 with MitoTracker Red), or nucleus (PCC = −0.25 with Hoechst) (Figure 3D). In addition, ER-proRed^{+} HeLa cells exhibited null red fluorescence (Figure 3D), reflecting nonfluorescent state of ROX-lactam moiety of ER-proRed in ER as proposed in Figure 1. Taken together, these results demonstrated stringent selectivity of ER-proRed for ER.

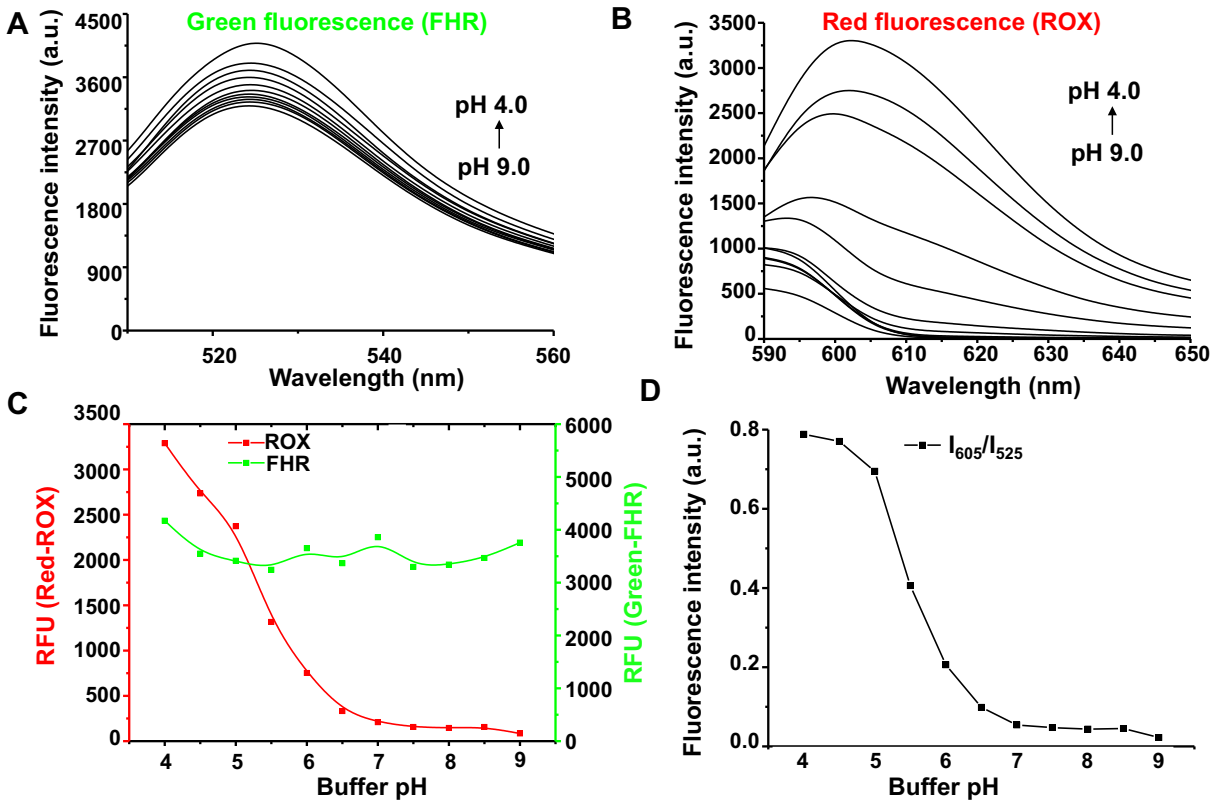

Figure 2. Optical property of ER-proRed. (A-B) Fluorescence emission of ER-proRed. ER-proRed was added to PBS buffer (10 mM, pH 4.0–9.0) containing 30% DMSO to a final concentration of 10 μM. These aqueous samples were analyzed for fluorescence emission using λ_{ex} = 495 nm for FHR and λ_{ex} = 585 nm for ROX. (C) pH titration curve of ER-proRed. The curve was plotted using fluorescence emission of FHR (I_{525} nm) and that of ROX (I_{605} nm) over pH. (D) Ratios of red to green fluorescence intensity (I_{605} nm/I_{525} nm).

Lysosomal acidity-triggered red fluorescence of ER-proRed in starved cells

With the selectivity for ER and acidity-triggered red fluorescence, we were keen to determine whether ER-proRed could be used to detect reticulophagy. As reticulophagy could be induced by amino acid starvation [13,14], HeLa cells pretreated with ER-proRed were starved in Hanks' balanced salt solution (HBSS) free of amino acids for 6 h to trigger reticulophagy. For comparison, we also starved HeLa cells expressing ss-RFP-GFP-KDEL [5,10,17], a ratiometric protein reporter exhibiting enhanced red-to-green emission at acidic settings. We observed massive red puncta across ss-RFP-GFP-KDEL$^+$ cells independent of starvation, and moderate increase in red-to-green fluorescence ratios upon starvation (Figure 4A), showing its low sensitivity to detect reticulophagy. In contrast, bright red signals were generated in starved ER-proRed$^+$ cells whereas such signals were very dim in control cells free of starvation (Figure 4B), suggesting reticulophagy mediated switch-on red fluorescence. Furthermore, the red dots in ER-proRed$^+$ cells colocalized with LysoTracker Blue (Figure 4B), A dye specific for lysosomes. Statistical analysis showed red fluorescence is 15-fold higher in starved cell than that in control cells (Figure 4C), consolidating high sensitivity of ER-proRed for reticulophagy detection. We then treated starved ER-proRed$^+$ cells with bafilomycin A_1 (Baf-A1) to neutralize lysosomes [35]. Baf-A1 caused loss of red fluorescence (Figure 4D), proving lysosomal acidity dependent red fluorescence of ER-proRed. The response of ER-proRed to starvation-induced reticulophagy was also confirmed in diverse cell lines including A-549, B16F10, RAW264.7 and U-2OS (Fig. S2). Combined, these findings show that the probe is activated by lysosomal acidity to give intense red fluorescence in reticulophagy.

Reticulophagy dependent turn-on red fluorescence of ER-proRed in live cells

To validate the dependence of fluorescence activation of ER-proRed on reticulophagy, ER-proRed$^+$ cells were starved in HBSS supplemented with chloroquine diphosphate (CQ). No red fluorescence could be identified in starved cells treated with CQ (Figure 5). As CQ prevents binding of autophagosomes to lysosomes [36], failed probe activation in starved cells is ascribed to blockade of ER-proRed into lysosomes by CQ. This supports co-delivery of ER-proRed together with ER into lysosomes in reticulophagy and red fluorescence generated thereof, reflecting dependence of probe activation on reticulophagy.

RETREG1 and TEX264 are ER-resident membrane receptor engaged in selective reticulophagy [9,10,13]. As overex-

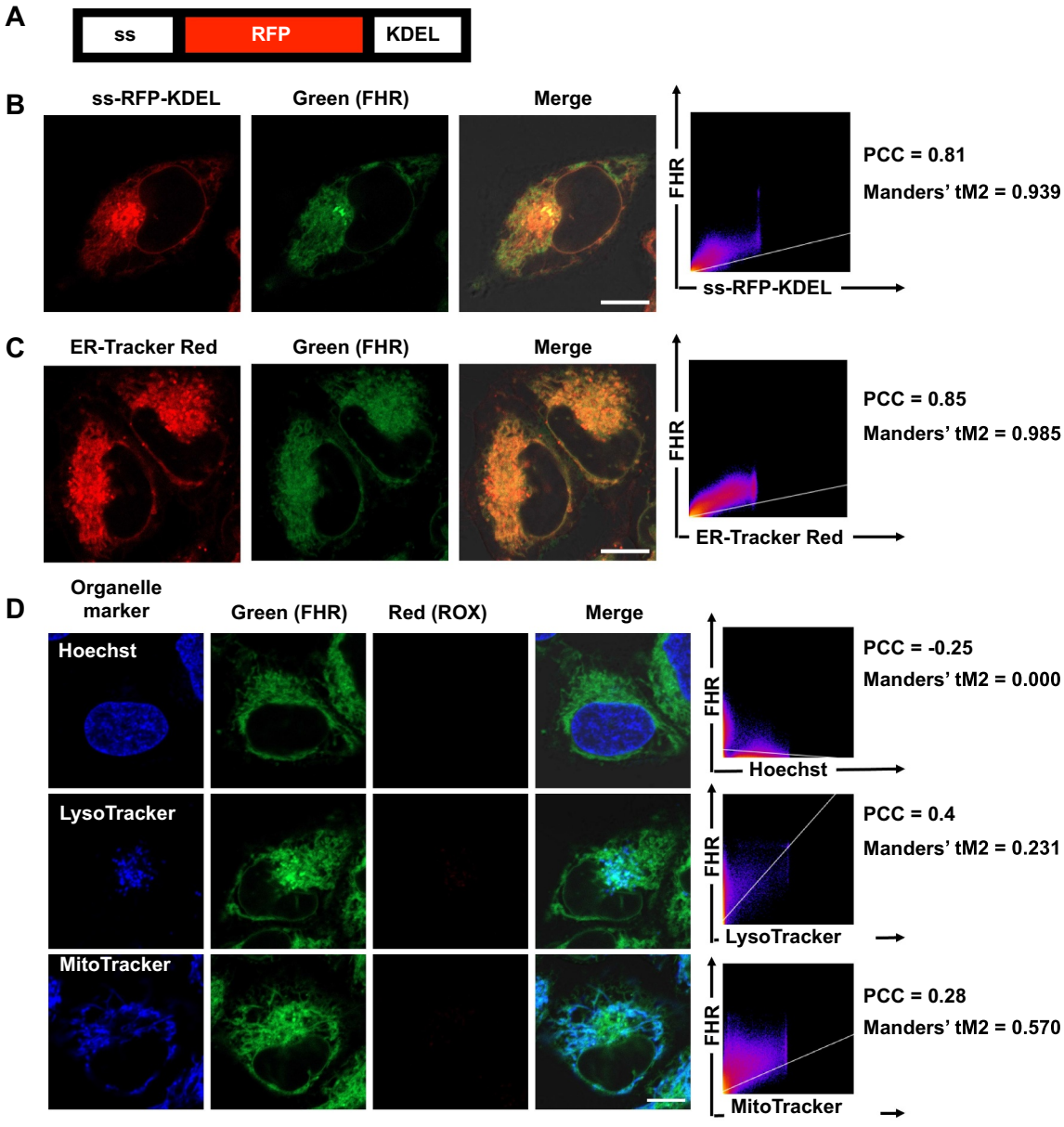

Figure 3. Selectivity of ER-proRed for ER. (A) Schematic for construction of ss-RFP-KDEL featuring red fluorescent protein flanked with N-terminal ER signal sequence of calreticulin (ss) and C-terminal KDEL peptide for retention in ER. (B) Colocalization of ss-RFP-KDEL with ER-proRed. ss-RFP-KDEL^{+} HeLa cells were stained with ER-proRed (5 μM) for 1 h at 37°C, washed with PBS for three times, and then visualized by confocal microscopy. (C) Colocalization of ER-Tracker Red with ER-proRed. HeLa cells prestained with ER-Tracker Red (2 μM, 30 min) were stained with ER-proRed (5 μM) for 1 h at 37°C. The cells were then washed with PBS and visualized by confocal microscopy. (D) Selectivity of ER-proRed for ER over other organelles. HeLa cells pretreated with ER-proRed were stained with hoechst (5 μg/μl, 20 min), LysoTracker Blue (1 μM, 30 min), or MitoTracker Blue (1 μM, 10 min), respectively. These cells were rinsed with PBS for three times, and then visualized by confocal microscopy. Scale bar: 10 μm.

pression of RETREG1 or TEX264 has been reported to induce reticulophagy, and to further verify fidelity of ER-proRed to reticulophagy, we overexpressed HA-F-RETREG1 or HA-TEX264 in HeLa cells (Fig. S3A). Both cell samples were stained with ER-proRed and then maintained in fresh cell culture medium for 6 h to allow basal reticulophagy. Very dim red fluorescence was generated in wild type HeLa cells after 6 h post-incubation (Figure 6A, C), due to low levels of basal reticulophagy during this 6 h incubation. In contrast, null at initial stage of cell culturing, strong red signals were identified in HA-RETREG1^{+} and HA-TEX264^{+} HeLa cells after 6 h culturing (Figure 6A, C). Red signals in cells over-expressing HA-RETREG1 or HA-TEX264 over wild type cells were also verified by flow cytometric analysis (Figure 6B). Reticulophagy boosted by these overexpressed reticulophagic receptors is consistent with previous observations [9,10,13]. Combined, the fidelity of ER-proRed to reticulophagy was established by red fluorescence that was abolished in CQ-blocked autophagy and yet dramatically enhanced by over-expressed receptors for reticulophagy.

Shown to be suitable for reticulophagy imaging, a time course study was performed to examine ER-proRed for un-activated rhodamine signal in ER of restive HeLa cells as well as activated rhodamine fluorescence in lysosomes of cells overexpressing reticulophagic receptors. We observed red fluorescence in ER in normal HeLa cells remains dim up to

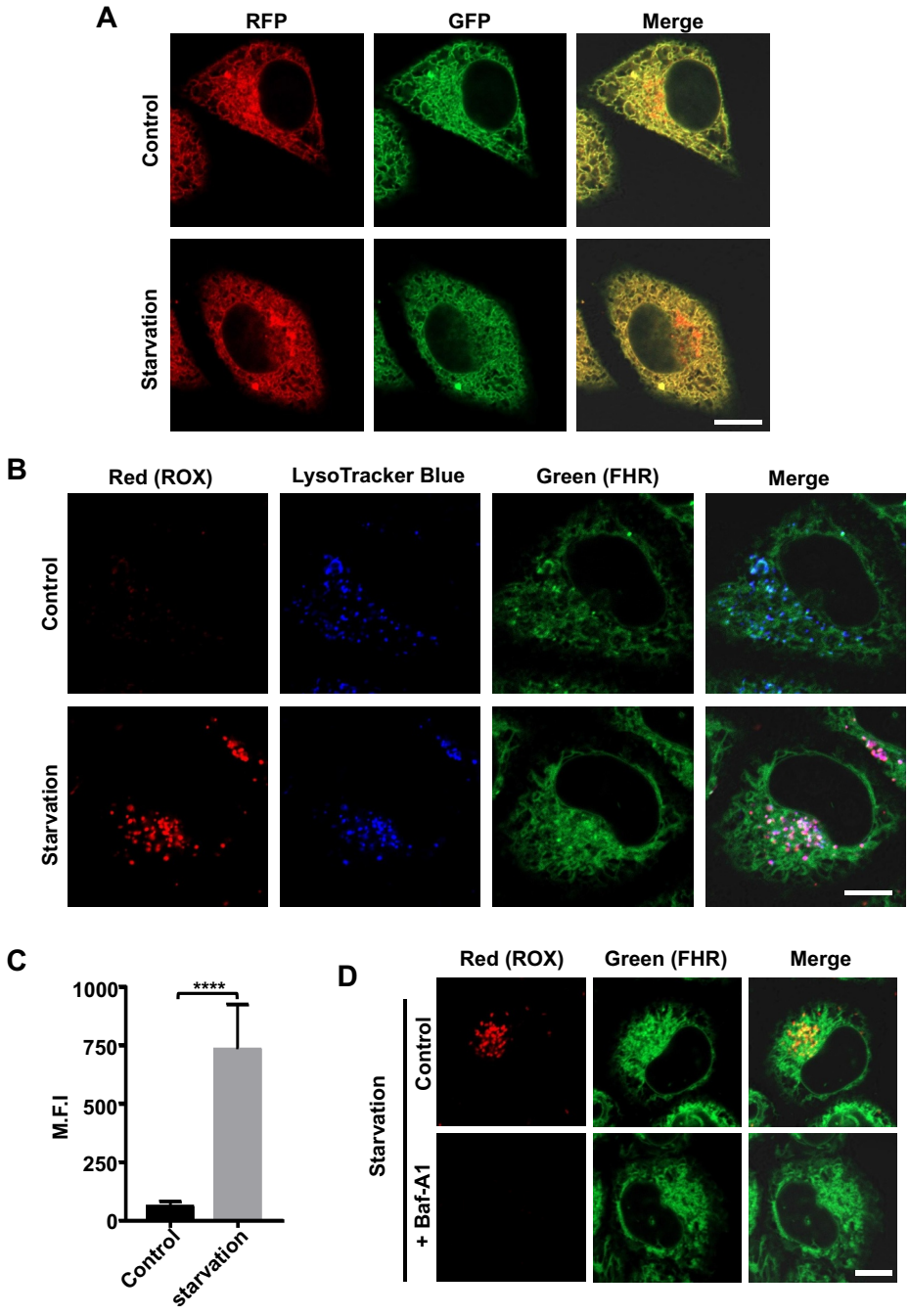

Figure 4. Sensitive fluorescence-on imaging of starvation-induced reticulophagy with ER-proRed. (A) Reticulophagy imaging with a classical fluorescent protein reporter. ss-RFP-GFP-KDEL^{+} HeLa cells were incubated for 6 h in DMEM (control) or HBSS (starvation) and then visualized by confocal microscopy. (B) Fluorescence-on imaging of reticulophagy with ER-proRed. HeLa cells co-stained with ER-proRed (5 μM, 1 h) and LysoTracker Blue (1 μM, 30 min) were incubated for 6 h in DMEM (control) or HBSS prior to confocal microscopic analysis. (C) Quantitation of red fluorescence in ER-proRed^{+} cells before and after starvation. Fluorescence intensity per cell was quantified by imagJ. mean ± SD, n = 20. ****, $P < 0.0001$ (t test). (D) Lysosomal acidity-mediated turn-on red fluorescence in ER-proRed^{+} cells upon starvation. ER-proRed^{+} HeLa cells were incubated for 6 h in HBSS supplemented with Baf-A1 (25 nM), or no addition (control). These cells were analyzed by confocal microscopy. Scale bar: 10 μm.

12 h whereas red signal occurred in lysosomes of RETREG1^{+} or TEX264^{+} cells at 4 h post incubation was constantly bright during 4–12 h post-incubation (Fig. S3B). These results show that the rhodamine signal is unactivated in ER and yet remains constantly bright in acidic lysosomes, showing the suitability of ER-proRed for live-cell imaging. Photobleaching often compromises the use of synthetic dyes in bioimaging. As such, HeLa cells stained with ER-proRed or commercial ER-Tracker Green were exposed to constant laser illumination, respectively. Time-lapse imaging showed that green fluorescence of ER-proRed decayed gradually upon laser illumination in a pattern similar to ER-Tracker Green whereas ER-proRed maintained higher levels of red fluorescence over ER-Tracker Green in starved cells (Fig. S1B-E). Lastly, we observed that that no obvious cytotoxicity was identified in cells with ER-proRed dosed up to 20 μM (Fig. S1F). The superior photo-stability of the red fluorescence and low probe cytotoxicity are beneficial for long term optical tracking

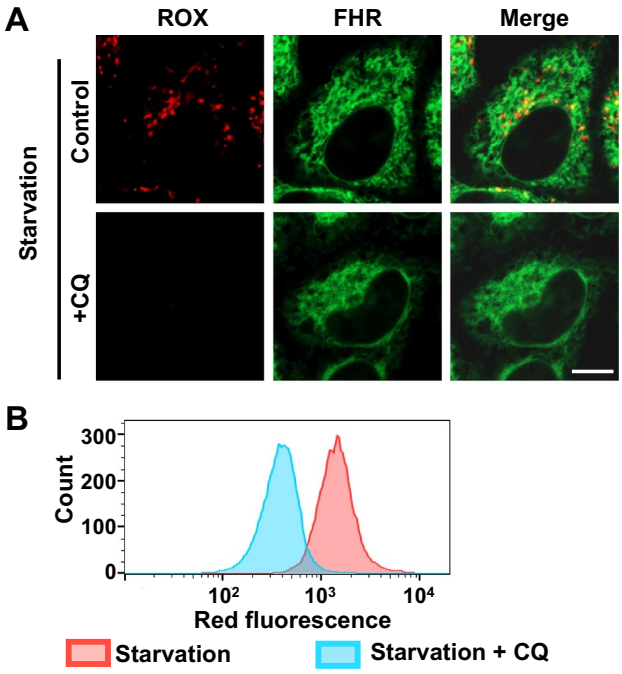

Figure 5. Blockade on fusion of autophagosomes with lysosomes suppressed fluorescence activation of ER-proRed in cell starvation. HeLa cells prestained with ER-proRed (5 μM, 1 h) were incubated for 6 h in HBSS supplemented with CQ (10 μM) or no addition (control). These cells were analyzed by confocal microscopy (A) or flow cytometry (B) for intracellular green and red fluorescence of ER-proRed. Scale bar: 10 μm.

of reticulophagy in live cells. Collectively, these results suggest the suitability of ER-proRed for live-cell imaging.

Identification of reticulophagy inducers with ER-proRed

With the sensitive imaging for reticulophagy and the lack of ER-inducers reported to date, we first applied ER-proRed to HeLa cells stressed with rapamycin, resveratrol, oligomycin, or CCCP. No reticulophagy could be identified in cells treated with rapamycin (an inhibitor of mTORC1) [37,38], rotenone (an inhibitor of NADH oxidase [39]), resveratrol (an inhibitor of mTOR), oligomycin (an inhibitor of ATP synthase), or CCCP which is a mitochondrial uncoupler and leads to AMPK activation and Parkin-dependent mitophagy [40] (Fig. S4C). These results showed that these widely used cell stressors were incapable of inducing reticulophagy.

We then assayed reticulophagy in HeLa cells stressed with thapsigargin [41,42] or tunicamycin [43] that have been reported to trigger ER stress by activating the unfolded protein response (UPR). We found that, despite altered ER morphology, no red signals could be observed in ER-proRed$^+$ HeLa cells incubated with thapsigargin or tunicamycin as compared to control cells (Fig. S4A, B). Failure of reticulophagy in response to thapsigargin or tunicamycin was also confirmed in ss-RFP-GFP-KDEL$^+$ HeLa cells (Fig. S4D). These observations are consistent with previous studies suggesting that no general autophagy or reticulophagy was

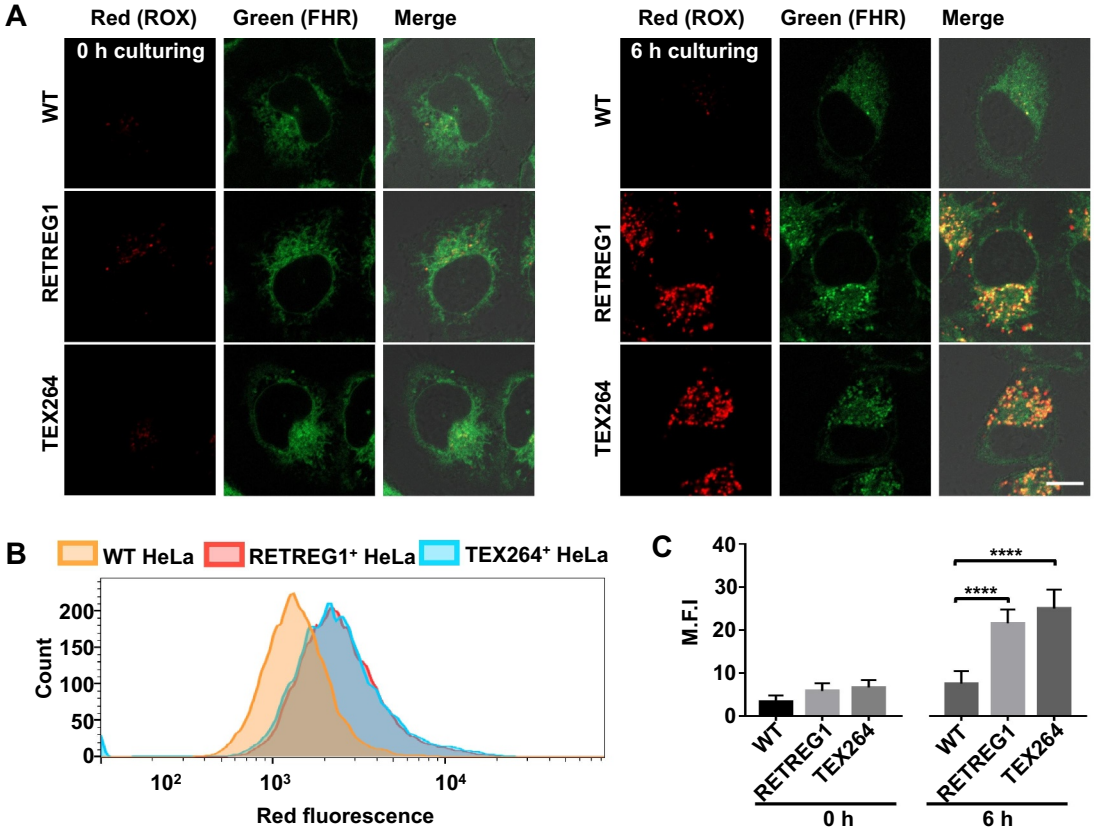

Figure 6. Reticulophagic receptors enhance fluorescence activation of ER-proRed. Wild-type (WT), HA-RETREG1$^+$ and HA-TEX264$^+$ HeLa cells were incubated with ER-proRed (5 μM) for 1 h at 37°C, incubated in fresh DMEM for 6 h, and then analyzed by confocal microscopy (A) or flow cytometry (B). Flow cytometric assays were performed using λ_{ex} = 561 nm and λ_{em} = 571–601 nm for red fluorescence, n = 10,000. (C) Quantification on intracellular red fluorescence in HA-RETREG1$^+$, HA-TEX264$^+$, or WT HeLa cells with ER-proRed. Red fluorescence intensity per cell was quantified by imageJ. mean ± SD, n = 20. ****, $P < 0.0001$ (t test). Scale bar: 10 μm.

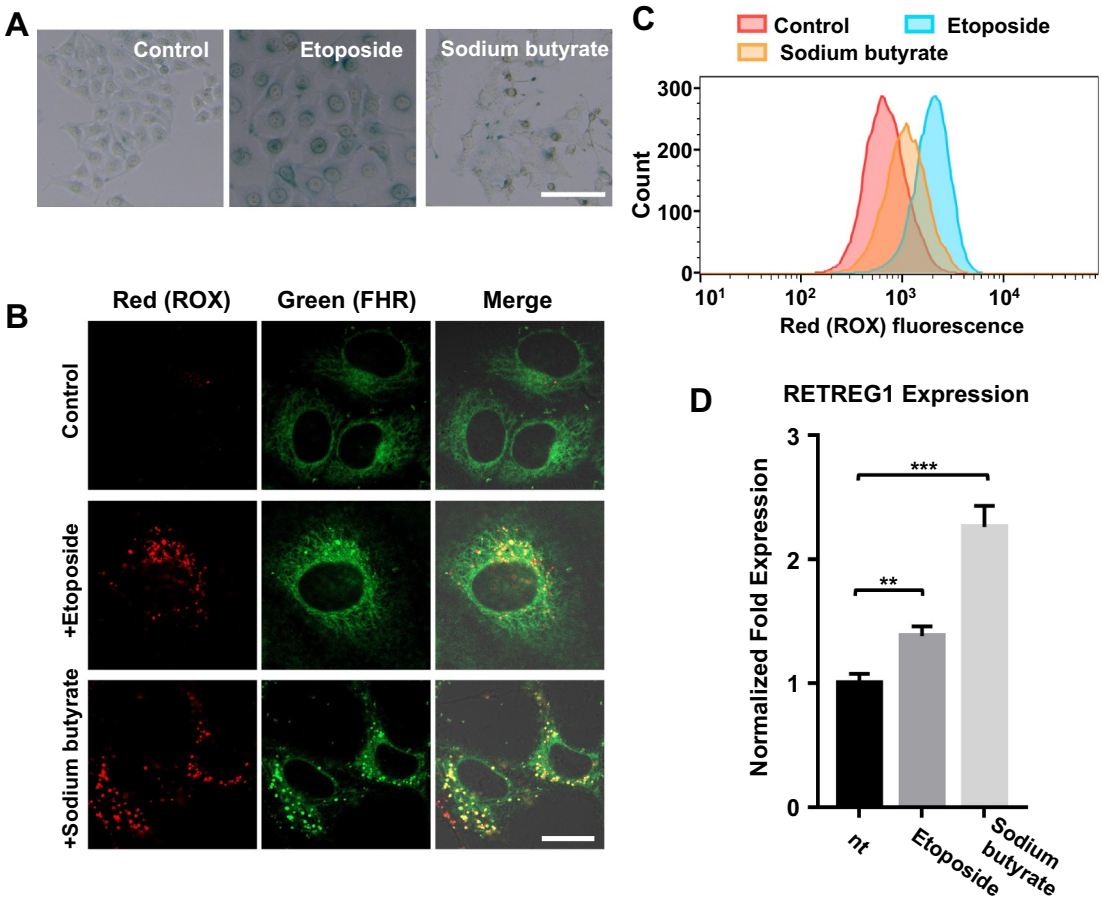

Figure 7. Reticulophagy induced by DNA damaging agents. (A) Bright field micrographs on SA-GLB1/β-gal staining of cells treated with DNA damaging agents. MCF-7 cells were incubated with DMEM containing etoposide (10 μM), or sodium butyrate (10 mM) for 24 h at 37°C to induce cellular senescence. These cells were then stained with X-gal. Cells cultured in DMEM free of addition were used as the control. Scale bar: 100 μm. (B/C) Detection of reticulophagy induced with DNA damaging agents with ER-proRed. MCF-7 cells pretreated with etoposide, or sodium butyrate were cultured with ER-proRed (5 μM, 1 h), washed with PBS, and then maintained in fresh DMEM for 6 h prior to analysis by confocal microscopy (B) or flow cytometry (C). Scale bar: 20 μm. (D) mRNA levels of RETREG1 in MCF-7 cells treated with etoposide or sodium butyrate. MCF-7 cells cultured for 24 h with DMEM containing etoposide (10 μM), sodium butyrate (10 mM) or no addition (nt) in DMEM were analyzed by qPCR. mean ± SD, n = 4. **, P = 0.0047. ***, P = 0.0009 (t test).

stimulated by UPR activation with thapsigargin or tunicamycin [14]. To assess whether reticulophagy could occur in post-ER stress recovery, HeLa cells were cultured for 12 h with thapsigargin, tunicamycin or cyclopiazonic acid (CPA) to induce UPR. These cells were washed to remove extracellular inducers and then analyzed with ER-proRed at 6 h post-UPR. Only tunicamycin-treated cells, but not thapsigargin or CPA treated cells, showed increased red signals compared to control cells (Fig. S5A, B, C). Independently, we observed slight reticulophagy induced by tunicamycin in ss-RFP-GFP-KEDL$^+$ HeLa cells under identical conditions (Fig. S5D). These data showed occurrence of reticulophagy during recovery of ER-stress induced by tunicamycin.

General autophagy has been reported to increase in senescence induced upon genomic DNA damaging [44]. Cellular senescence, a stable arrest of the cell cycle, accumulates with aging and could promote age-related diseases [45]. Whether reticulophagy occurs under such conditions remains unclear. Etoposide [46] and sodium butyrate [47,48] cause DNA damages and induce cellular senescence through different mechanisms [49]. To discern whether reticulophagy arises in response to DNA damaging agents, we administered etoposide and sodium butyrate to MCF-7 cells, respectively. After validating cell senescence by positive staining with SA-GLB1 /β-gal, a biomarker of senescent cells [50,51] (Figure 7A), we applied ER-proRed to these cells and observed pronounced red signals in cells treated with etoposide or sodium butyrate over control cells (Figure 7B-C). Although less sensitive, this pattern was observed in ss-RFP-GFP-KEDL$^+$ HeLa cells (Fig. S6). With reticulophagy revealed by ER-proRed, we then performed RNA-seq analysis on transcriptome of MCF-7 cells subjected to etoposide or sodium butyrate and found that at least one reticulophagy receptor, RETREG1, is transcriptionally upregulated in cells treated with both agents over control cells. Quantitative RT-PCR analysis further verified elevated RETREG1 mRNA expression in MCF-7 cells treated with etoposide or sodium butyrate (Figure 7D), which is consistent with the reported role of RETREG1 as a reticulophagy regulator. Reticulophagy observed in the presence of etoposide or sodium butyrate warrants future work to explore DNA-damage induced reticulophagy further. Taken together, these data validate the applicability of ER-

proRed to evaluate reticulophagy inducers, which are potential pharmacological agents.

Conclusion

Reticulophagy plays an important role in ER homeostasis and ER quality control by lysosomal degradation of excess or damaged ER. Protein reporters such as mKeima have been widely used to assay various autophagy events by enhanced red-to-green signals [10,17,52]. Complementing these systems that require construct of reporter-expressing cell lines by plasmid transfection, we herein described a ready-to-use small molecular probe (ER-proRed) that overrides the need for plasmid transfection and generation of a stable cell line expressing reticulophagy reporter system. ER-proRed features an ER-targeted entity with green fluorescence and an entity of ROX-lactam prone to lysosomal acidity triggered red fluorescence. Trapped in ER, ER-proRed could be delivered into acidic lysosomes together with ER in reticulophagy, whereby giving rise to intense red fluorescence. The turn-on red signals triggered by reticulophagy in principle allowed detection of reticulophagy with higher sensitivity, and were utilized to evaluate various cell stressors for their capability to induce reticulophagy. Exemplified by ER-proRed, molecular probes integrating an appropriate organelle tracker with a profluorophore activatable to lysosomal acidity might be extended to detect autophagy of other organelles such as lipid droplets and Golgi apparatus, and thus offer valuable tools for autophagy research.

Materials and methods

Cell lines, plasmids and reagents

HeLa (ATCC®, CCL-2™), B16F10 (ATCC®, CRL-6475™), A-549 (ATCC®, CCL-185), U-2OS (ATCC®, HTB-96), RAW264.7 (ATCC®, TIB-71) and MCF-7 (ATCC®, HTB-22™) cells were obtained from American Type Culture Collection. All cell lines were maintained in Dulbecco's modified Eagle's medium (DMEM; GIBCO, 11995500CP) supplemented with 10% fetal bovine serum (Thermo, A3160901), 2 mM L-glutamine (Millipore, TMS-002-C), 100 IU penicillin (Gibco, 15,140,122), and 100 mg/mL streptomycin (Sangon, A610494-0050) at 37°C in a humidified incubator under 5% CO_2, unless specified. Bafilomycin A_1 (Baf-A1; S1413), rapamycin (S1039) and oligomycin (S1478) were purchased from Selleck. Pennsylvania green (BD00808725) was purchased from Bidepharm. ROX was purchased from Bioluminor (D0405). Chloroquine diphosphate (HY-17589) was purchased from MedChemExpress. Etoposide (E1383), CCCP (C2759), cyclopiazonic acid (C1530) and resveratrol (501–36-0) were obtained from Sigma. Rotenone (sc-203,242) was purchased from Santa Cruz Biotechnology. Sodium butyrate (479,725) was purchased from J&K Scientific. X-gal (A600083-0001) was purchased from Sangon Biotech. All other chemicals were purchased from Sigma unless specified. The antibodies used in this study were: Anti-RETREG1 /FAM134B (Proteintech, 21,537-1-AP), anti-GAPDH (ABclonal, AC002) and anti-HA (GNI Japan, GNI4110-H-B).

HA-RETREG1/FAM134B-, HA-TEX264-, ss-RFP-KDEL- and ss-RFP-GFP-KDEL-expressing plasmid were used for producing recombinant lentiviruses, respectively. Full-length cDNA of *TEX264* (NP_001123356) or *RETREG1* (NP_061873) was cloned into BamHI and XhoI sites of the lentiviral vector pBOB-CMV (Addgene, 134,275; deposited by Dr. Jiahuai Han's Lab, Xiamen University) using the ExoIII-assisted ligase-free cloning method [53], 3 × HA were also used for tagging. To generate pBOB-CMV-ss-RFP-GFP-KDEL, the minimal CMV promotor and DNA sequences encoding the signal sequence of CALR and RFP-GFP-KDEL were subcloned into pBOB backbone vector. The same method was used for the generation of pBOB-CMV-ss-RFP-KDEL. Recombinant lentiviruses were generated in 293 T cells (ATCC®, ACS-4500™) in the presence of helper plasmids (pMDLg, Addgene, 12,253; pRSV-RE, Addgene, 12,251; pVSV-G, Addgene, 138,479, all the plasmids were deposited by Dr. Jiahuai Han's Lab, Xiamen University) using a calcium phosphate precipitation method [54] All plasmids were verified by DNA sequencing. Expression of HA-TEX264, HA-RETREG1, ss-RFP-KDEL, ss-RFP-GFP-KDEL was validated by GFP/RFP fluorescence or western blot.

Microscopy

The fluorescence spectra were performed on SpectraMax M5 (Molecular Device). Confocal fluorescence microscopy imaging was performed on Zeiss LSM 980 using the following parameters. Hoechest and LysoTracker Blue: laser wavelength = 405 nm, laser power = 57 μW, Gain = 700 V. FHR and GFP: laser wavelength = 488 nm, laser power = 58 μW, Gain = 600 V. tagRFP: laser wavelength = 543 nm, laser power = 61 μW, Gain = 760 V. ROX: laser wavelength = 594 nm, laser power = 17 μW, Gain = 600 V. LysoTracker Deep Red: laser wavelength = 643 nm, laser power = 53 μW, Gain = 500 V. pixel size = 0.066 μm, line accumulation = 150 μs, averaging number = 8.

Graph was generated by GraphPad Prism7 software. Flow cytometry analysis was performed on BD Fortessa. The fluorescence emission intensity of FHR was recorded by FITC filter (515–545 nm) using excitation wavelength of 488 nm while that of ROX was recorded by PE (571–601 nm) using excitation wavelength of 561 nm. 10,000 Cells gated under identical conditions were analyzed and the data were processed by FlowJo V10. All the cells analyzed by confocal microscopy were seeded in 35 mm glass-bottom cell culture dishes purchased from NEST, Wuxi.

pH titration

A stock soluiton of ER-proRed in DMSO was added to phosphate-buffered saline (PBS; 137.0 mM NaCl, 2.7 mM KCl, 10 mM Na_2HPO4, 2.0 mM KH_2PO_4, pH 7.4) containing 30% DMSO (pH: 4.0, 4.5, 5.0, 5.5, 6.0, 6.5, 7.0, 7.5, 8.0, 8.5, 9.0) to a final concentration of 10 μM. Fluorescence spectra were recorded using λ_{ex} = 495 nm for FHR and λ_{ex} = 585 nm for ROX. pH titration curves of the ER-proRed was plotted using fluorescence emission of FHR (I_{525} nm) and that of ROX (I_{605} nm) over pH.

Probe selectivity for ER in ss-RFP-KEDL$^+$ HeLa cells

ss-RFP-KEDL$^+$ HeLa cells were cultured with ER-proRed (5 μM) for 1 h in DMEM at 37°C. The cells were washed with PBS for three times and then analyzed by confocal fluorescence microscopy.

Comparison of ER-proRed and ER-Tracker Red

HeLa cells were cultured with ER-Tracker Red (2 μM; beyotime, C1041) for 30 min in stain buffer at 37°C. The cells were then washed with PBS three times and incubated with DMEM containing ER-proRed (5 μM) for 1 h at 37°C. The cells were then analyzed by confocal fluorescence microscopy.

Selectivity of ER-proRed for ER over other organelles

HeLa cells were cultured in DMEM containing 5 μM ER-proRed for 1 h at 37°C. The cells were then washed with PBS for three times and then incubated with DMEM containing Hoechst (2 μg/ml, 20 min), LysoTracker (1 μM, 30 min), and MitoTracker (1 μM, 10 min), respectively at 37°C. The cells were then imaged by confocal fluorescence microscopy.

Fluorescence-on detection of reticulophagy induced by starvation with ER-proRed

HeLa cells cultured with ER-proRed (5 μM, 1 h) and Lysotracker Blue (1 μM, 30 min) in DMEM at 37°C. Then the cells were washed with PBS three times and further maintained in nutrient-rich medium (DMEM containing 10% fetal calf serum) or starvation conditions (HBSS) for 6 h at 37°C. The cells were then analyzed by confocal microscopy. Rhodamine fluorescence intensity per cell was quantified by imageJ [55].

Imaging of reticulophagy with ss-RFP-KDEL

ss-RFP-GFP-KDEL$^+$ HeLa cells were incubated for 6 h in DMEM (control) or HBSS (starvation) at 37°C and then analyzed by confocal microscopy.

Tracking of reticulophagy with ER-proRed in different cell lines

A-549, B16F10, RAW264.7 or U-2OS cells were cultured for 1 h in DMEM containing ER-proRed (5 μM) at 37°C. The cells were washed with PBS three times and then maintained in DMEM (control) or HBSS (starvation) for 6 h at 37°C. The cells were then analyzed by confocal microscopy.

Cytotoxicity of ER-proRed

HeLa cells were cultured in a 96-well cell culture plate containing ER-proRed (0, 1, 2, 5, 10, 20 μM) for 60 min. These cell samples were washed with PBS for three times and then further cultured in fresh DMEM for 0 h, 24 h, or 48 h. The resultant cells were determined for cell viability by cell count kit 8 (MCE, hy-k0301) assay.

Loss in rhodamine fluorescence of starved HeLa cells stained with Baf-A1 or CQ

HeLa cells were cultured for 1 h in DMEM containing ER-proRed (5 μM) at 37 °C. The cells were washed with PBS three times and then maintained for 6 h in HBSS or HBSS containing Baf-A1 (25 nM) or CQ (10 μM). The cells were then analyzed by confocal microscopy or flow cytometry.

Tracking of reticulophagy in RETREG1 or TEX264 expressing cells by ER-proRed

RETREG1$^+$, TEX264$^+$ or WT HeLa cells were cultured for 1 h in DMEM containing ER-proRed (5 μM) at 37°C. The cells were washed with PBS for three times and then maintained in DMEM for 6 h at 37°C. The cells were then analyzed by confocal microscopy or flow cytometry. Rhodamine fluorescence intensity per cell was quantified by imagJ.

Time course monitoring on red fluorescence of ER-proRed in control or cells overexpressing reticulophagic receptors

WT, HA-RETREG1$^+$ or HA-TEX264$^+$ HeLa cells were cultured for 1 h in DMEM containing ER-proRed (5 μM) at 37°C. The cells were washed with PBS, and then maintained in fresh DMEM. The cells were then analyzed by confocal microscopy at different time points (0, 4, 8, 12 h).

Photo-stability of ER-proRed and ER-Tracker Red

HeLa cells were incubated with ER-proRed (5 μM) or ER-Tracker Green (1 μM; Beyotime, C1042S) for 60 min at 37°C under 5% CO_2 in DMEM. In parallel, HeLa cells pre-cultured with ER-proRed (5 μM) were further maintain for 6 h in HBSS free of amino acid. Then cells were subjected to constant laser illumination and then analyzed by confocal fluorescence microscopy or flow cytometry at indicated time points (0 – 55 min). (λ_{ex} = 488 nm for green fluorescence, λ_{ex} = 594 nm for red fluorescence). The images were analyzed using ZEN blue 2 and ImageJ software. Z-Stack: 5 Slices (920 nm).

Determine reticulophagy occurrence in HeLa cells under varied stressed conditions

HeLa cells were cultured for 1 h in DMEM containing ER-proRed (5 μM) at 37°C. The cells were washed with PBS for three times and then maintained in DMEM containing thapsigargin (1 μM; Sigma, T9033-1 MG), tunicamycin (0.5 μM; Tocris, Cat. No. 3516), rapamycin (1 μM), rotenone (10 μM), resveratrol (10 μM), oligomycin (10 μM), carbonyl cyanide m-chlorophenylhydrazone (CCCP; 10 μM) or no addition for 6 h at 37°C. The cells were then analyzed by confocal fluorescence microscopy or flow cytometry.

Post-UPR assay with ER-proRed

HeLa cells were cultured for 12 h in DMEM containing thapsigargin (1 μM), tunicamycin (0.5 μg/ml), CPA (10 μM; Sigma, C1530-5 MG) at 37°C, respectively. The cells were then

stained with 5 μM ER-proRed for 1 h and further incubated in fresh DMEM for 6 h, and then analyzed by confocal microscopy or flow cytometry.

Post-UPR with ss-RFP-GFP-KEDL$^+$ HeLa cells

ss-RFP-GFP-KEDL$^+$ HeLa cells were cultured for 12 h in DMEM containing thapsigargin (1 μM), tunicamycin (0.5 μg/ml), CPA (10 μM) at 37°C respectively. The cells were washed with PBS for three times and further incubated in fresh DMEM for 6 h. The cells were then analyzed by confocal microscopy.

SA-GLB1/β-gal staining of senescent cells

MCF-7 cells were cultured for 24 h in DMEM containing etoposide (10 μM), sodium butyrate (10 mM) or no addition at 37°C. The cells were then stained according to the previously described method [50,51]. In brief, cells grown on plates were washed with PBS, fixed in 2% formaldehyde containing 0.2% glutaraldehyde for 5 min at room temperature, and washed again with PBS. Then, cells were incubated overnight at 37°C without CO_2 in a freshly prepared staining buffer (1 mg/ml 5-bromo-4-chloro-3-indolyl-β-galactopyranoside (X-gal), 40 mM citric acid/ sodium phosphate, pH 6.0, 5 mM potassium ferrocyanide, 5 mM potassium ferricyanide, 150 mM NaCl, and 2 mM $MgCl_2$) for 24 h. The cells were then imaged by bright field micrographs.

Detection of reticulophagy induced by etoposide or sodium butyrate with ER-proRed

MCF-7 cells were cultured at 37°C for 24 h in DMEM containing etoposide (10 μM), sodium butyrate (10 mM) or no addition. The cells were washed with PBS and then cultured for 1 h in DMEM containing ER-proRed (5 μM) at 37°C. The cells were then washed again with PBS for three times and then further maintained in DMEM for 6 h at 37°C. The resultant cells were analyzed by confocal fluorescence microscopy or flow cytometry.

Detection of reticulophagy induced by etoposide or sodium butyrate with ss-RFP-GFP-KEDL$^+$ cells

ss-RFP-GFP-KEDL$^+$ MCF-7 cells were cultured at 37°C for 24 h in DMEM containing etoposide (10 μM), sodium butyrate (10 mM) or no addition. The cells were washed with PBS for three times and further incubated in fresh DMEM for 6 h. The cells were then analyzed by confocal microscopy.

Real time q-PCR quantification of RETREG1 and GAPDH mRNA expression

Total RNA was extracted from cells with TRIzol (Accurate Biotechnology, AG21102) according to the manufacturer's instructions. cDNA was prepared with M-MLV reverse transcriptase and oligo-dT primers. Quantitative PCR analysis was performed using SYBR Green reagent (Vazyme, Q711-02) along with gene-specific primers. All the results were analyzed by relative quantification and normalization to the RNA level of *GAPDH*. The following primer sequences were used:

GAPDH-F: 5′-TGATGACATCAAGAAGGTGGTG-3′;
GAPDH-R: 5′-TGTGAGGAGGGGAGATTCAG-3′;
RETREG1-F: 5′-GTCTCAGAGGTATCCTGGACTG-3′;
RETREG1-R: 5′-TTCCTCACTGGGTCGGTCAAGA-3′.

Statistical analyses

All values in the figures are expressed as the mean ± standard deviation (SD). The statistical significance of the differences between the two groups was determined using the Student's t test.

Acknowledgments

We thank Narong Yang for helpful discussion.

Disclosure statement

No potential conflict of interest was reported by the authors.

Funding

This work was supported by grants from National Natural Science Foundation of China (NSFC) (22177096), NSFC (81788101), National Key R&D Program of China (2020YFA0803500), and the CAMS Innovation Fund for Medical Science (2019-I2M-5-062).

Supporting information

Available on synthesis and characterization of the compounds, cell cytotoxicity, Images of western blotting, cell imaging, and cytotoxicity etc.

References

[1] Schwarz DS, Blower MD. The endoplasmic reticulum: structure, function and response to cellular signaling. Cell Mol Life Sci. 2016;73:79–94.
[2] Yang M, Luo S, Wang X, et al. ER-Phagy: a new regulator of ER homeostasis. Front Cell Dev Biol. 2021;9:1–10.
[3] He L, Qian X, Cui Y. Advances in ER-Phagy and its diseases relevance. Cells. 2021;10:2328–2352.
[4] Wilkinson S. ER-phagy: shaping up and destressing the endoplasmic reticulum. FEBS J. 2019;286:2645–2663.
[5] Chino H, Mizushima N. ER-Phagy: quality control and turnover of endoplasmic reticulum. Trends Cell Biol. 2020;30:384–398.
[6] Reggiori F, Molinari M. ER-phagy: mechanisms, regulation and diseases connected to the lysosomal clearance of the endoplasmic reticulum. Physiol Rev. 2022;102(3):1393–1448.
[7] Liao Y, Duan B, Zhang Y, et al. Excessive ER-phagy mediated by the autophagy receptor FAM134B results in ER stress, the unfolded protein response, and cell death in HeLa cells. J Biol Chem. 2019;294:20009–20023.
[8] Chiramel AI, Dougherty JD, Nair V, et al. FAM134B, the selective autophagy receptor for endoplasmic reticulum turnover, inhibits replication of Ebola virus strains Makona and Mayinga. J Infect Dis. 2016;214:S319–S325.
[9] Khaminets A, Heinrich T, Mari M, et al. Regulation of endoplasmic reticulum turnover by selective autophagy. Nature. 2015;522:354–358.
[10] Chino H, Hatta T, Natsume T, et al. Intrinsically disordered protein TEX264 mediates ER-phagy. Mol Cell. 2019;74:909–921 e906.

[11] Hu S, Ye H, Cui Y, et al. AtSec62 is critical for plant development and is involved in ER-phagy in Arabidopsis thaliana. J Integr Plant Biol. 2020;62:181–200.
[12] Fumagalli F, Noack J, Bergmann Timothy J, et al. Translocon component Sec62 acts in endoplasmic reticulum turnover during stress recovery. Nat Cell Biol. 2016;18:1173–1184.
[13] Ferro-Novick S, Reggiori F, Jl B. ER-Phagy, ER homeostasis, and ER quality control: implications for disease. Trends Biochem Sci. 2021;46:630–639.
[14] Liang JR, Lingeman E, Luong T, et al. A genome-wide ER-phagy screen highlights key roles of mitochondrial metabolism and ER-resident UFMylation. Cell. 2020;180:1160–1177 e1120.
[15] Chen Q, Xiao Y, Chai P, et al. ATL3 is a tubular ER-Phagy receptor for GABARAP-mediated selective autophagy. Curr Biol. 2019;29:846–855.e846.
[16] Grumati P, Morozzi G, Hölper S, et al. Full length RTN3 regulates turnover of tubular endoplasmic reticulum via selective autophagy. eLife. 2017;6:e25555.
[17] Mizushima N, Murphy LO. Autophagy assays for biological discovery and therapeutic development. Trends Biochem Sci. 2020;45:1080–1093.
[18] Anding AL, Baehrecke EH. Cleaning house: selective autophagy of organelles. Dev Cell. 2017;41:10–22.
[19] Otomo T, Yoshimori T. Lysophagy: a method for monitoring lysosomal rupture followed by autophagy-dependent recovery. Methods Mol Biol. 2017;1594:141–149.
[20] Iwashita H, Torii S, Nagahora N, et al. Live cell imaging of mitochondrial autophagy with a novel fluorescent small molecule. ACS Chem Biol. 2017;12:2546–2551.
[21] Li X, Hu Y, Li X, et al. Mitochondria-immobilized near-infrared ratiometric fluorescent pH probe to evaluate cellular mitophagy. Anal Chem. 2019;91:11409–11416.
[22] Shi Y, Zou X, Wen S, et al. An organelle-directed chemical ligation approach enables dual-color detection of mitophagy. Autophagy. 2021;17:3475–3490.
[23] Zhang W, Kwok RT, Chen Y, et al. Real-time monitoring of the mitophagy process by a photostable fluorescent mitochondrion-specific bioprobe with AIE characteristics. Chem Commun (Camb). 2015;51:9022–9025.
[24] Katayama H, Hama H, Nagasawa K, et al. Visualizing and modulating mitophagy for therapeutic studies of neurodegeneration. Cell. 2020;181:1176–1187 e1116.
[25] Lee MH, Park N, Yi C, et al. Mitochondria-immobilized pH-sensitive off-on fluorescent probe. J Am Chem Soc. 2014;136:14136–14142.
[26] McWilliams TG, Prescott AR, Allen GF, et al. Mito-QC illuminates mitophagy and mitochondrial architecture in vivo. J Cell Biol. 2016;214:333–345.
[27] Sun N, Yun J, Liu J, et al. Measuring in Vivo mitophagy. Mol Cell. 2015;60:685–696.
[28] Fujisawa A, Tamura T, Yasueda Y, et al. Chemical profiling of the endoplasmic reticulum proteome using designer labeling reagents. J Am Chem Soc. 2018;140:17060–17070.
[29] Meinig JM, Fu L, Peterson BR. Synthesis of fluorophores that target small molecules to the endoplasmic reticulum of living mammalian cells. Angew Chem Int Ed Engl. 2015;54:9696–9699.
[30] Dadina N, Tyson J, Zheng S, et al. Imaging organelle membranes in live cells at the nanoscale with lipid-based fluorescent probes. Curr Opin Chem Biol. 2021;65:154–162.
[31] Shi Y, Zou X, Wen S, et al. An organelle-directed chemical ligation approach enables dual-color detection of mitophagy. Autophagy. 2021;17:3475–3490.
[32] Xue Z, Zhao H, Liu J, et al. Imaging lysosomal pH alteration in stressed cells with a sensitive ratiometric fluorescence sensor. ACS Sens. 2017;2:436–442.
[33] Xue Z, Zhao H, Liu J, et al. Responsive hetero-organelle partition conferred fluorogenic sensing of mitochondrial depolarization. Chem Sci. 2017;8:1915–1921.
[34] CellLight™ ER-RFP.2022 Apr 22. BacMam 2.0, C10591, thermo fisher scientific. https://www.thermofisher.cn/order/catalog/product/C10591#/C10591
[35] Harada M, Shakado S, Sakisaka S, et al. Bafilomycin A1, a specific inhibitor of V-type H+-ATPases, inhibits the acidification of endocytic structures and inhibits horseradish peroxidase uptake in isolated rat sinusoidal endothelial cells. Liver. 1997;17:244–250.
[36] Mauthe M, Orhon I, Rocchi C, et al. Chloroquine inhibits autophagic flux by decreasing autophagosome-lysosome fusion. Autophagy. 2018;14:1435–1455.
[37] Rangaraju S, Verrier JD, Madorsky I, et al. Rapamycin activates autophagy and improves myelination in explant cultures from neuropathic mice. J Neurosci. 2010;30:11388–11397.
[38] Edwards SR, Wandless TJ. The rapamycin-binding domain of the protein kinase mammalian target of rapamycin is a destabilizing domain. J Biol Chem. 2007;282:13395–13401.
[39] Li N, Ragheb K, Lawler G, et al. Mitochondrial complex I inhibitor rotenone induces apoptosis through enhancing mitochondrial reactive oxygen species production. J Biol Chem. 2003;278:8516–8525.
[40] Goldsby RA, Heytler PG. Uncoupling of oxidative phosphorylation by carbonyl cyanide phenylhydrazones. ii. effects of carbonyl cyanide m-chlorophenylhydrazone on mitochondrial respiration. Biochemistry. 1963;2:1142–1147.
[41] Abdullahi A, Stanojcic M, Parousis A, et al. Modeling acute ER stress in Vivo and in vitro. Shock. 2017;47:506–513.
[42] Geiszt M, Káldi K, Szeberényi JB, et al. Thapsigargin inhibits Ca2 + entry into human neutrophil granulocytes. Biochem J. 1995;305 (Pt 2):525–528.
[43] Guha P, Kaptan E, Gade P, et al. Tunicamycin induced endoplasmic reticulum stress promotes apoptosis of prostate cancer cells by activating mTORC1. Oncotarget. 2017;8:68191–68207.
[44] Goehe RW, Di X, Sharma K, et al. The autophagy-senescence connection in chemotherapy: must tumor cells (self) eat before they sleep? J Pharmacol Exp Ther. 2012;343:763–778.
[45] Arnould T, Vankoningsloo S, Renard P, et al. CREB activation induced by mitochondrial dysfunction is a new signaling pathway that impairs cell proliferation. EMBO J. 2002;21:53–63.
[46] te Poele RH, Okorokov AL, Jardine L, et al. DNA damage is able to induce senescence in tumor cells in vitro and in Vivo1. Cancer Res. 2002;62:1876–1883.
[47] Terao Y, Nishida J, Horiuchi S, et al. Sodium butyrate induces growth arrest and senescence-like phenotypes in gynecologic cancer cells. Int J Cancer. 2001;94:257–267.
[48] Xiao H, Hasegawa T, Miyaishi O, et al. Sodium butyrate induces NIH3T3 cells to senescence-like state and enhances promoter activity of p21WAF/CIP1 in p53-independent manner. Biochem Biophys Res Commun. 1997;237:457–460.
[49] Petrova NV, Velichko AK, Razin SV, et al. Small molecule compounds that induce cellular senescence. Aging Cell. 2016;15:999–1017.
[50] Debacq-Chainiaux F, Erusalimsky JD, Campisi J, et al. Protocols to detect senescence-associated beta-galactosidase (SA-betagal) activity, a biomarker of senescent cells in culture and in vivo. Nat Protoc. 2009;4:1798–1806.
[51] Dimri GP, Lee X, Basile G, et al. A biomarker that identifies senescent human cells in culture and in aging skin in vivo. Proc Natl Acad Sci U S A. 1995;92:9363–9367.
[52] Liang JR, Lingeman E, Ahmed S, et al. Atlastins remodel the endoplasmic reticulum for selective autophagy. J Cell Biol. 2018;217:3354–3367.
[53] Li C, Evans RM. Ligation independent cloning irrespective of restriction site compatibility. Nucleic Acids Res. 1997;25:4165–4166.
[54] Jordan M, Schallhorn A, Wurm FM. Transfecting mammalian cells: optimization of critical parameters affecting calcium-phosphate precipitate formation. Nucleic Acids Res. 1996;24:596–601.
[55] Schindelin J, Arganda-Carreras I, Frise E, et al. Fiji: an open-source platform for biological-image analysis. Nat Methods. 2012;9:676–682.